# 6 Models for thin structures

by Peter Howell

## 6.1 Longitudinal displacement of a bar

As a first illustrative example, let us consider longitudinal waves propagating along a thin bar with uniform cross-section area $A$. We consider a short segment of the bar between some arbitrary point $x$ and $x+\delta x$, where $x$ measures longitudinal distance along the bar. The mass of this segment is $\rho A\delta x$, where $\rho$ is the volume density of the bar, and the dominant force it experiences consists of the tensions $T$ exerted on each of its faces by the sections of the bar on either side, as illustrated in Figure 6.1. Denoting the longitudinal displacement by $u(x,t)$, we thus obtain Newton's second law in the form

$$T(x+\delta x,t)-T(x,t)=\rho A\delta x\frac{\partial^2 u}{\partial t^2}(x,t). \tag{6.1}$$

In the limit $\delta x\to 0$, this reduces to the partial differential equation

$$\frac{\partial T}{\partial x}=\rho A\frac{\partial^2 u}{\partial t^2}. \tag{6.2}$$

To close the problem, we now need a constitutive relation between $T$ and $u$. On physical grounds, we might expect $T$ to be proportional to the stretch $\partial u/\partial x$, by analogy with Hooke's law. Motivated by the exact static solution obtained in Section 2, we postulate the relation

$$T=EA\frac{\partial u}{\partial x}, \tag{6.3}$$

where

$$E=\frac{\mu(3\lambda+2\mu)}{\lambda+\mu} \tag{6.4}$$

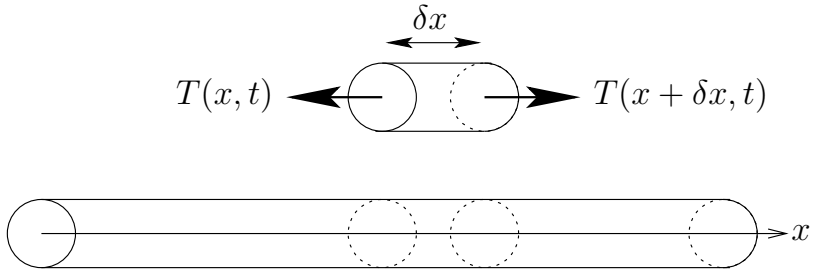


Figure 6.1: Schematic of a uniform bar showing the forces acting on a small segment of length $\delta x$.

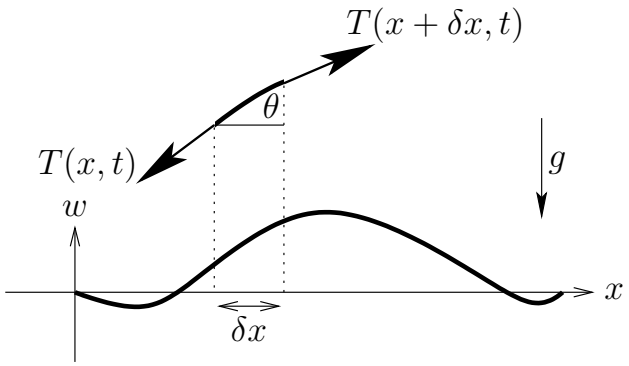


Figure 6.2: Schematic of an elastic string showing the forces acting on a small segment of length $\delta x$.

again denotes Young's modulus. By substituting (6.3) into (6.2), we find that $u(x,t)$ satisfies the wave equation

$$E\frac{\partial^2 u}{\partial x^2} = \rho\frac{\partial^2 u}{\partial t^2}. \tag{6.5}$$

which says that longitudinal waves in the bar travel with speed $\sqrt{E/\rho}$. Since $E < \lambda + 2\mu$, these waves travel slower than longitudinal $P$-waves. Typical boundary conditions are that $u$ or the axial force $EA\partial u/\partial x$ should be prescribed at each end of the bar and, of course, $u$ and $\partial u/\partial t$ need to be given at $t = 0$.

We should point out that various implicit assumptions underly the derivation given above. We have assumed, for example, that the longitudinal displacement $u$ is uniform in each cross-section of the bar, and that the constitutive relation (6.3) holds although its derivation in Section 2 was performed only under static conditions. Neither of these assumptions is exactly true in practice, reflecting the fact that solutions of (6.5) are not exact solutions of the Navier equations. Intuitively, we expect (6.5) to be a good approximate model when the bar is thin and the displacement is small, specifically if $u \ll \sqrt{A} \ll L$, where $L$ is the length of the bar. With considerably more effort, it can be derived systematically by nondimensionalising the Navier equation and boundary conditions and taking an appropriate asymptotic limit.

## 6.2 Transverse displacements of a string

Before deriving a model for the transverse displacements of a beam, let us remind ourselves briefly of the corresponding derivation for an elastic string, which is characterised by the fact that the only internal force that it can support is a tension $T$ acting in the tangential direction. Assuming that gravity $g$ acts transversely to the string, as illustrated in Figure 6.2, the net force experienced by a small segment of undisturbed length $\delta x$ is

$$\left[T\begin{pmatrix}\cos\theta\\ \sin\theta\end{pmatrix}\right]_x^{x+\delta x} + \begin{pmatrix}0\\ -\varrho g\end{pmatrix}\delta x,$$

where $\varrho$ denotes the line density.

Under the assumption that the transverse displacement $w(x,t)$ is small compared to the length of the string, we can approximate the angle $\theta$ between the string and the $x$-axis by

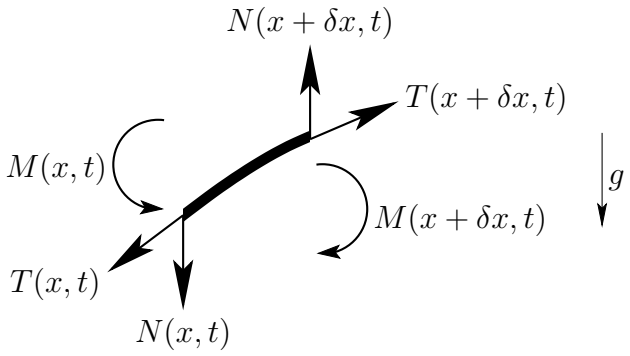


Figure 6.3: Schematic showing the forces and moments acting on a small segment of an elastic beam.

$\theta \sim \partial w/\partial x \ll 1$ and hence use the leading-order approximations

$$\sin\theta \sim \frac{\partial w}{\partial x}, \qquad\qquad \cos\theta \sim 1. \tag{6.6}$$

At the same time, we suppose that there is no longitudinal displacement so that the acceleration is just $\partial^2 w/\partial t^2$ in the vertical direction. By applying Newton's second law to the segment and letting $\delta x \to 0$, we thus obtain the equations

$$\frac{\partial T}{\partial x} = 0, \qquad\qquad T\frac{\partial^2 w}{\partial x^2} - \varrho g = \varrho\frac{\partial^2 w}{\partial t^2}. \tag{6.7}$$

Hence we find again that the displacement satisfies the wave equation and that the tension $T$ must be spatially uniform. Usually $T$ is assumed to be a known constant although, in principle, it may be a function of time, for example while a guitar string is being tuned. Common experience suggests that a string is unable to withstand a compressive longitudinal force and hence that $T$ should be positive. We can make the same observation on mathematical grounds by noting that (6.7b) would change type from hyperbolic to elliptic if $T$ were negative, and hence cease to be well-posed as an initial-value problem.

## 6.3 Transverse displacements of a beam

### 6.3.1 Derivation of the beam equation

Now let us consider how to extend the model derived above to describe an elastic beam. In contrast with a string, a beam can support an appreciable transverse *shear force* $N$ as well as the tension $T$, as illustrated in Figure 6.3; for convenience $N$ is defined to act perpendicular to the $x$-axis. Again considering small, purely transverse displacements, we obtain the equations

$$\frac{\partial T}{\partial x} = 0, \qquad\qquad T\frac{\partial^2 w}{\partial x^2} + \frac{\partial N}{\partial x} - \varrho g = \varrho\frac{\partial^2 w}{\partial t^2}. \tag{6.8}$$

Now our task is to relate $N$ to $w$, and we start by performing a moment balance on the segment shown in Figure 6.3. When doing so, we suppose that each section of the beam exerts on its neighbours a *bending moment* $M$ about the $y$-axis, as well as the tangential and

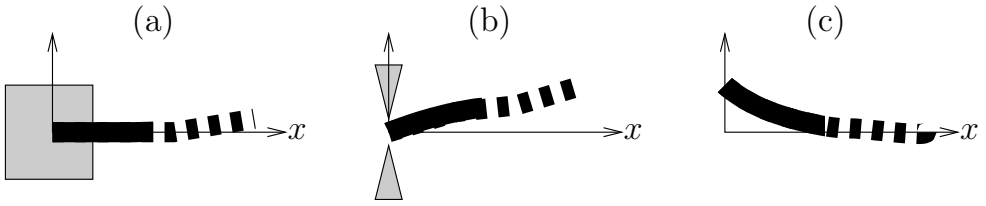


Figure 6.4: Schematic of the end of a beam under (a) clamped, (b) simply supported and (c) free conditions.

normal force components $T$ and $N$. Conservation of angular momentum about the point $x$ leads to the equation

$$-M(x+\delta x,t)+M(x,t)+\delta x N(x+\delta x,t)=\varrho g\frac{\delta x^2}{2}+\hat{I}\frac{\partial^2\theta}{\partial t^2}, \tag{6.9}$$

where $\theta\approx\partial w/\partial x$ is once again the small slope of the beam and the moment of inertia of the segment about its end is given by $\hat{I}=\varrho(\delta x)^3/3$. When we let $\delta x\to 0$, the right-hand side of (6.9) is thus negligible and we are left with

$$-\frac{\partial M}{\partial x}+N=0. \tag{6.10}$$

Finally, we need a constitutive relation for $M$. It is a practical experience, for example when bending a flexible ruler, that applying an increasing moment to a beam results in an increasing curvature. For small displacements, this suggests a constitutive relation of the form

$$M=-B\frac{\partial^2 w}{\partial x^2}, \tag{6.11}$$

where $B$ is a constant known as the *bending stiffness*. Again we can use a simple exact solution of the Navier equations from Section 2 to pose the relation

$$B=EI, \qquad \text{where} \quad I=\iint_A z^2\,\mathrm{d}y\mathrm{d}z \tag{6.12}$$

is the moment of inertia of the cross section $A$ about the $y$-axis.

Postulating that the constitutive relation (6.11) still holds under dynamic conditions, we combine (6.8)–(6.12), to obtain the *beam equation*

$$-EI\frac{\partial^4 w}{\partial x^4}+T\frac{\partial^2 w}{\partial x^2}-\varrho g=\varrho\frac{\partial^2 w}{\partial t^2}. \tag{6.13}$$

Evidently, (6.13) reduces to (6.7) as the bending stiffness $EI$ tends to zero.

### 6.3.2 Boundary conditions

On physical grounds we expect to need to specify $w$ and $\partial w/\partial t$ at $t=0$, as for a string. However, since (6.13) has four $x$-derivatives rather than two, we might anticipate that it requires *two* boundary conditions at each end of the beam, in contrast with a string. If, for

example, a beam is *clamped* as shown in Figure 6.4(a), then both $w$ and $\partial w/\partial x$ would be prescribed at the clamp; in the case illustrated

$$w = \frac{\partial w}{\partial x} = 0. \tag{6.14}$$

Alternatively, we could envisage a *simply supported* beam end, as shown in Figure 6.4(b), where the displacement is fixed without applying any moment, so that $w = M = 0$ and thus

$$w = \frac{\partial^2 w}{\partial x^2} = 0. \tag{6.15}$$

In the final example shown in Figure 6.4(c), the end of the beam is *free*. It therefore experiences no shear force or bending moment, and from (6.10) and (6.11) we deduce the boundary conditions

$$\frac{\partial^2 w}{\partial x^2} = \frac{\partial^3 w}{\partial x^3} = 0, \tag{6.16}$$

and in this case we must also have $T \equiv 0$.

### 6.3.3 Compression of a beam

One of the most dramatic new features of (6.16) compared with (6.7) is that we can now consider situations in which $T < 0$. We illustrate an unexpected new possibility that arises in such cases by considering steady displacements of a beam of length $L$ subject to negligible gravity. We suppose that the ends are clamped and subject to a compressive force $P = -T$ and zero transverse force. In this case (6.13) reduces to the ordinary differential equation

$$EI\frac{\mathrm{d}^4 w}{\mathrm{d}x^4} + P\frac{\mathrm{d}^2 w}{\mathrm{d}x^2} = 0, \tag{6.17a}$$

subject to the boundary conditions

$$\frac{\mathrm{d}w}{\mathrm{d}x} = \frac{\mathrm{d}^3 w}{\mathrm{d}x^3} = 0 \qquad \text{at} \quad x = 0, L. \tag{6.17b}$$

We can consider (6.17) as an *eigenvalue problem*. One possibility is always that the beam remains straight with $w \equiv$ const. but, if the applied force takes one of the discrete values

$$\frac{P}{EI} = \frac{n^2\pi^2}{L^2}, \tag{6.18}$$

where $n$ is an integer, then (6.17) admits the eigenfunction solution

$$w = A\cos\left(\frac{n\pi x}{L}\right), \tag{6.19}$$

where $A$ is a constant.

The first three such eigenfunctions are shown in Figure 6.5; these are the shapes that a beam can adopt as it *buckles* under a sufficiently large compressive force. The *amplitude* $A$ appears to be indeterminate, although we might expect it to to be a smoothly increasing function of the applied force. This is a deficiency of the model that will be addressed in §6.4.

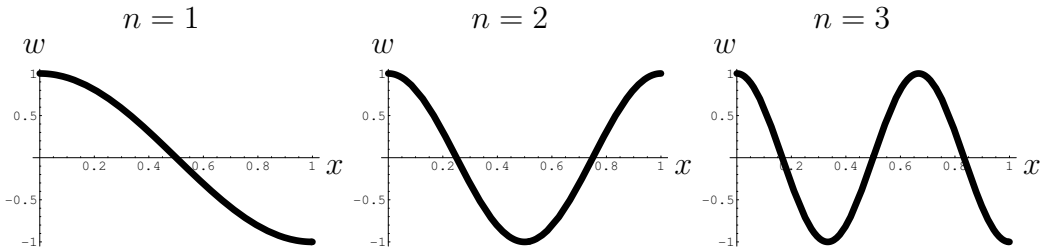


Figure 6.5: The first three buckling modes of a clamped elastic beam (with $a = 1$ and $L = 1$).

### 6.3.4 Waves on a beam

For the dynamic beam equation (6.13) with $g = 0$, we can seek travelling-wave solutions of the form

$$u = A\exp\bigl(\mathrm{i}(kx - \omega t)\bigr), \tag{6.20}$$

where the real part is assumed as usual, and hence obtain the dispersion relation

$$\varrho\omega^2 = EIk^4 + Tk^2. \tag{6.21}$$

Elastic waves on a beam are therefore dispersive, unlike $P$-waves, $S$-waves or waves on a string. This should not come as too much of a surprise, since we have already discovered that elastic waves are usually dispersive when boundaries are present.

For a beam under positive tension $T > 0$, waves with frequency $\omega$ can thus propagate with wavelength $2\pi/k$ provided

$$\frac{\omega}{k} = \sqrt{\frac{T}{\varrho}}\left(1 + \frac{EIk^2}{T}\right)^{1/2}. \tag{6.22}$$

Evidently this reduces to the dispersion relation for a string if the waves are long, with $k \ll \sqrt{T/EI}$. For a beam under compression, with $P = -T > 0$, wave-like solutions of (6.13) exist only if $k^2 > P/EI$. For smaller values of $k$, (6.21) leads to *complex* values of $\omega$, corresponding to solutions that grow exponentially in time. It follows that the beam is *unstable* to waves with wavelength larger than $2\pi\sqrt{EI/P}$, and we will investigate this further in §6.4.5.

## 6.4 Nonlinear beam theory

### 6.4.1 Derivation of the model

In equilibrium, it is surprisingly easy to generalise our derivation of linear beam theory in §6.3 to model large two-dimensional transverse displacements. We describe the deformation of the beam using arc-length $s$ along the centre-line and the angle $\theta(s)$ between the centre-line and the $x$-axis. As discussed above, we assume the centre-line to be inextensible to leading order, so that arc-length is conserved by the deformation and we can thus view $s$ as a Lagrangian coordinate that is fixed in the deforming beam. The transverse displacement is given parametrically by $x = x(s)$, $w = w(s)$, where

$$\frac{\mathrm{d}x}{\mathrm{d}s} = \cos\theta, \qquad\qquad \frac{\mathrm{d}w}{\mathrm{d}s} = \sin\theta. \tag{6.23}$$

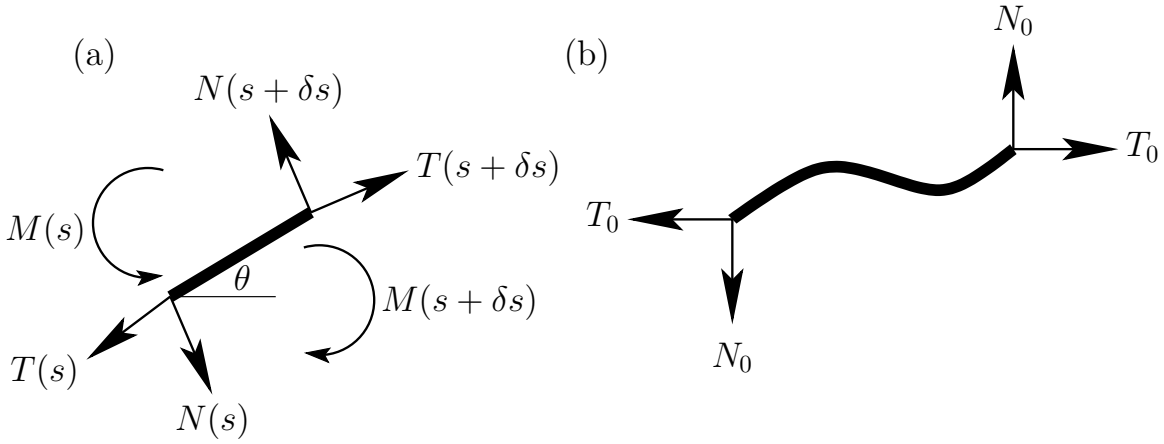


Figure 6.6: (a) Schematic of the forces and moments acting on a small segment of a beam. (b) Definition sketch showing the sign convention for the forces at the ends of the beam.

Now we balance forces and moments on a small segment of the beam as shown in Figure 6.6(a). We neglect inertia and body forces for the moment and note that $N$ is now defined to be the *normal*, rather than transverse, force; since $\theta$ is no longer assumed to be small this is a significant distinction. We thus obtain the equations

$$\frac{\mathrm{d}}{\mathrm{d}s}\left(T\cos\theta - N\sin\theta\right) = 0, \qquad \frac{\mathrm{d}}{\mathrm{d}s}\left(N\cos\theta + T\sin\theta\right) = 0, \qquad \frac{\mathrm{d}M}{\mathrm{d}s} - N = 0, \tag{6.24}$$

the first two of which simply show that the internal forces in the $x$- and $z$-directions are conserved. If a force $(T_0, N_0)$ is applied at the right-hand end, with an equal and opposite force at the left-hand end, as in Figure 6.6(b), it follows that

$$T = T_0\cos\theta + N_0\sin\theta, \qquad\qquad N = N_0\cos\theta - T_0\sin\theta. \tag{6.25}$$

As a constitutive relation we expect, as in §6.3, the bending moment to be proportional to the curvature which, for a nonlinear deflection, is given by $\mathrm{d}\theta/\mathrm{d}s$. Since we are considering small strains, we assume that the constant of proportionality is the same as in the linear case, that is

$$M = -EI\frac{\mathrm{d}\theta}{\mathrm{d}s}. \tag{6.26}$$

By collecting (6.24c), (6.25) and (6.26), we obtain the celebrated *Euler strut* equation

$$EI\frac{\mathrm{d}^2\theta}{\mathrm{d}s^2} + N_0\cos\theta - T_0\sin\theta = 0. \tag{6.27}$$

### 6.4.2 Boundary conditions

If we are given the applied force components $T_0$ and $N_0$, then we expect to impose two further boundary conditions (one at each end) on the second-order differential equation (6.27). Typical examples are clamped conditions, where we specify the angle $\theta$, or simple support, where there is zero bending moment and hence $\mathrm{d}\theta/\mathrm{d}s = 0$. Suppose, instead, that we are told the positions of the ends of the beam. Without loss of generality, we suppose the end $s = 0$

is fixed at the origin, and denote by $(X, Z)$ the position of the other end $s = L$, where $L$ is the length of the beam. We then deduce from (6.23) the conditions

$$X = \int_0^L \cos\theta(s)\,\mathrm{d}s, \qquad\qquad Z = \int_0^L \sin\theta(s)\,\mathrm{d}s, \tag{6.28}$$

from which we can in principle recover $T_0$ and $N_0$.

### 6.4.3 Linearisation

It is reassuring to confirm that the Euler strut model reduces to the linear beam theory derived in §6.3 for cases where the deflection is small. For small $\theta$, we can simplify the geometric relations (6.23) to lowest order to give

$$x = s, \qquad\qquad \frac{\mathrm{d}w}{\mathrm{d}x} = \theta, \tag{6.29}$$

and (6.27) thus becomes

$$EI\frac{\mathrm{d}^3 w}{\mathrm{d}x^3} + N_0 - T_0\frac{\mathrm{d}w}{\mathrm{d}x} = 0. \tag{6.30}$$

One further $x$-derivative reproduces the linear beam equation (6.13) in the absence of inertia and gravity.

### 6.4.4 Example: deflection of a diving board

Let us first consider the example, alluded to previously, of the steady deformation of a diving board. If the board is clamped horizontally at $s = 0$ and a downward load $F$ is applied to the other end, which is otherwise free, then we have $T_0 = 0$, $N_0 = -F$ and (6.27) becomes

$$EI\frac{\mathrm{d}^2\theta}{\mathrm{d}s^2} = F\cos\theta, \tag{6.31}$$

subject to

$$\theta(0) = 0, \qquad\qquad \frac{\mathrm{d}\theta}{\mathrm{d}s}(L) = 0. \tag{6.32}$$

Multiplying (6.31) through by $\mathrm{d}\theta/\mathrm{d}s$ and integrating once with respect to $s$, we obtain

$$\left(\frac{\mathrm{d}\theta}{\mathrm{d}s}\right)^2 = \frac{2F}{EI}\left(\sin\theta + \sin\alpha\right), \tag{6.33}$$

where $\alpha$ is shorthand for $-\theta(L)$. When taking the square root, we note that we expect $\mathrm{d}\theta/\mathrm{d}s$ to be negative and thus obtain the solution in parametric form as

$$\int_0^{-\theta} \frac{\mathrm{d}\phi}{\sqrt{\sin\alpha - \sin\phi}} = s\sqrt{\frac{2F}{EI}}. \tag{6.34}$$

It just remains to determine the angle $\alpha$ from the transcendental equation

$$\int_0^{\alpha} \frac{\mathrm{d}\phi}{\sqrt{\sin\alpha - \sin\phi}} = L\sqrt{\frac{2F}{EI}}, \tag{6.35}$$

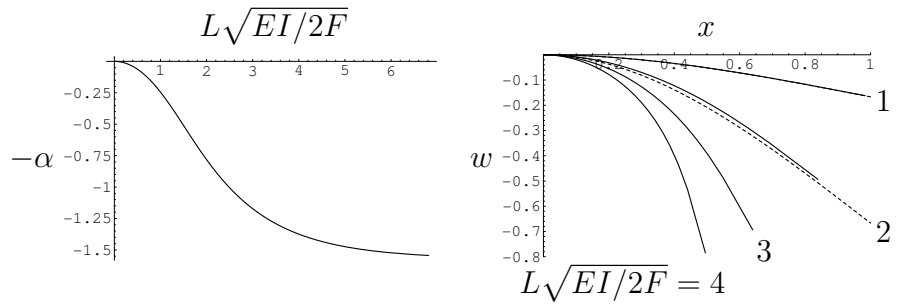


Figure 6.7: (a) Final angle $-\alpha$ of a diving board versus applied force parameter $L\sqrt{2F/EI}$. (b) Deflection of a diving board for various values of the force parameter; the dashed lines show the linearised solution.

which can be written in terms of so-called elliptic integrals. Given the applied force $F$, we have to solve (6.35) for $\alpha$ (numerically), and the deflection may then be reconstructed using (6.34) and (6.23).

In Figure 6.7(a), we plot the final angle $-\alpha$ as a function of the force parameter $L\sqrt{2F/EI}$. As the applied force increases, the angle decreases, tending towards $-\pi/2$. In Figure 6.7(b), we show the diving board profile corresponding to different applied forces, and we can see clearly how the force causes the deflection to increase.

For small applied forces, we would expect the linear equation (6.30) to be applicable. The linear model that describes our diving board is

$$EI\frac{\mathrm{d}^3 w}{\mathrm{d}x^3} = F, \qquad w(0) = \frac{\mathrm{d}w}{\mathrm{d}x}(0) = 0, \qquad \frac{\mathrm{d}^2 w}{\mathrm{d}x^2}(L) = 0, \tag{6.36}$$

and the solution is readily found to be

$$w = -\frac{F}{6EI}x^2(3L - x). \tag{6.37}$$

In Figure 6.7(b), (6.37) is plotted as dashed curves, and we see that there is excellent agreement with the full nonlinear model provided the deflections are reasonably small.

### 6.4.5 Weakly nonlinear theory and buckling

Now let us return to the buckling of an elastic beam, which we discussed previously in the linear case in §6.3. We focus on the model problem of a beam of length $L$, clamped at both ends, subject to a compressive force $P = -T_0$ and zero transverse force. We therefore have to solve

$$\frac{\mathrm{d}^2\theta}{\mathrm{d}s^2} + \frac{P}{EI}\sin\theta = 0, \tag{6.38a}$$

subject to the boundary conditions

$$\theta(0) = \theta(L) = 0. \tag{6.38b}$$

This is a *nonlinear* eigenvalue problem: $\theta \equiv 0$ is always a possibility, and we are seeking values of the applied force $P$ for which (6.38) admits nonzero solutions. Such solutions, if they exist, correspond to *buckling* of the beam.

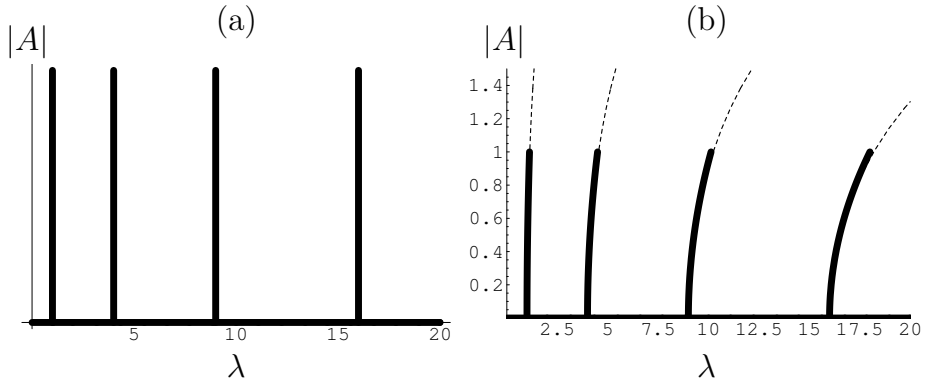


Figure 6.8: (a) Response diagram of the amplitude $\|\theta\|$ of the linearised solution (6.39) for a buckling beam versus the force parameter $\lambda$. (b) Corresponding response of the weakly nonlinear solution; the exact nonlinear solution is shown using dashed lines.

If $\theta$ is small, it is easy to show that (6.38) reduces to the linear eigenvalue problem (6.17) studied previously, and we can read off from (6.19) the solution

$$\theta = \begin{cases} A\sin\left(\dfrac{n\pi s}{L}\right) & \dfrac{L^2P}{\pi^2EI} = n^2, \\ 0 & \text{otherwise,} \end{cases} \tag{6.39}$$

where $n$ is any integer. Thus the amplitude $A$ of the solution is zero, unless $P$ takes one of a discrete set of critical values, in which case it is arbitrary. Hence buckling can only occur when

$$P = \pi^2\frac{EI}{L^2} \tag{6.40}$$

We can try to visualise this behaviour by plotting a *response diagram* of the magnitude of the solution

$$\|\theta\| = \max_{0<s<1}|\theta| = |A| \tag{6.41}$$

versus the control parameter

$$\lambda = \frac{L^2P}{\pi^2EI}. \tag{6.42}$$

The response diagram corresponding to (6.39) is shown in Figure 6.8(a); exactly the same diagram would have resulted had we used any other sensible norm $\|\theta\|$ instead of (6.41).

There are several problems with the solution (6.39). When $\lambda = n^2$, where $n$ is an integer, the solution is not unique, since its amplitude is indeterminate. Also, if the applied force slightly exceeds one of the critical values, we would expect on physical grounds that the buckling would continue, while Figure 6.8(a) indicates that the solution instantly reverts to $\theta \equiv 0$. These criticisms can be answered by noting that, if we follow one of the branches $\lambda = n^2$, then $\theta$ will eventually increase to the point where the linearisation of (6.38) is no longer valid.

We therefore need to reintroduce the nonlinearity to resolve the behaviour when $\lambda$ is close to $n^2$. To do this systematically requires the use of asymptotic analysis, and we must first

nondimensionalise the model. The angle $\theta$ is already dimensionless, but it is convenient to define

$$\theta = \delta\Theta, \tag{6.43}$$

where $\Theta$ is order unity and $\delta$ is a small positive parameter that characterises the smallness of $\theta$. We also set $s = L\xi$ and thus obtain the dimensionless model

$$\frac{\mathrm{d}^2\Theta}{\mathrm{d}\xi^2} + \pi^2\lambda\frac{\sin(\delta\Theta)}{\delta} = 0, \qquad \theta(0) = \theta(1) = 0, \tag{6.44}$$

where $\lambda$ is again the dimensionless parameter defined by (6.42). We focus on a neighbourhood of $\lambda = n^2$ by writing

$$\lambda = n^2 + \varepsilon\lambda_1, \tag{6.45}$$

where $\varepsilon$ is a fixed small positive number and $\lambda_1$ is a control parameter which parametrises the difference between $\lambda$ and $n^2$.

We thus have *two* small parameters in the problem: the amplitude $\delta$ of the solution and the deviation $\varepsilon$ of $\lambda$ from its critical value. The vital step is to find a relation between these two parameters that yields a balance between the compressive loading, characterised by $\varepsilon$, and the nonlinearity, characterised by $\delta$, and the correct choice leads to a so-called *weakly nonlinear* theory. If we use the assumed smallness of $\delta$ to expand the sine in (6.44), we obtain the *Duffing equation*

$$\frac{\mathrm{d}^2\Theta}{\mathrm{d}\xi^2} + \pi^2\left(n^2 + \varepsilon\lambda_1\right)\left(\Theta - \delta^2\frac{\Theta^3}{6} + \cdots\right) = 0, \tag{6.46}$$

and we clearly see that the required balance is obtained by choosing

$$\delta = \sqrt{\varepsilon}. \tag{6.47}$$

Before doing any further calculation, we can already infer from this that the amplitude of the solution will vary as the square root of the excess loading.

After making the choice (6.47), we write $\Theta$ as an asymptotic expansion of the form

$$\Theta \sim \Theta_0(\xi) + \varepsilon\Theta_1(\xi) + \cdots. \tag{6.48}$$

By substituting (6.48) into (6.46) and equating successive powers of $\varepsilon$, we find that

$$\frac{\mathrm{d}^2\Theta_0}{\mathrm{d}\xi^2} + n^2\pi^2\Theta_0 = 0, \qquad \Theta_0(0) = \Theta_0(1) = 0, \tag{6.49a}$$

$$\frac{\mathrm{d}^2\Theta_1}{\mathrm{d}\xi^2} + n^2\pi^2\Theta_1 = -\pi^2\lambda_1\Theta_0 + n^2\pi^2\frac{\Theta_0^3}{6}, \qquad \Theta_1(0) = \Theta_1(1) = 0. \tag{6.49b}$$

The general solution of (6.49a) is

$$\Theta_0 = A_0\sin(n\pi\xi), \tag{6.50}$$

and we seem to have made very little progress from (6.39). However, when we examine the problem for $\Theta_1$, we find that (6.49b) has no solutions unless the right-hand side satisfies a solvability condition, namely

$$\int_0^1 \left(\lambda_1\Theta_0 - n^2\frac{\Theta_0^3}{6}\right)\sin(n\pi\xi)\,\mathrm{d}\xi = 0. \tag{6.51}$$

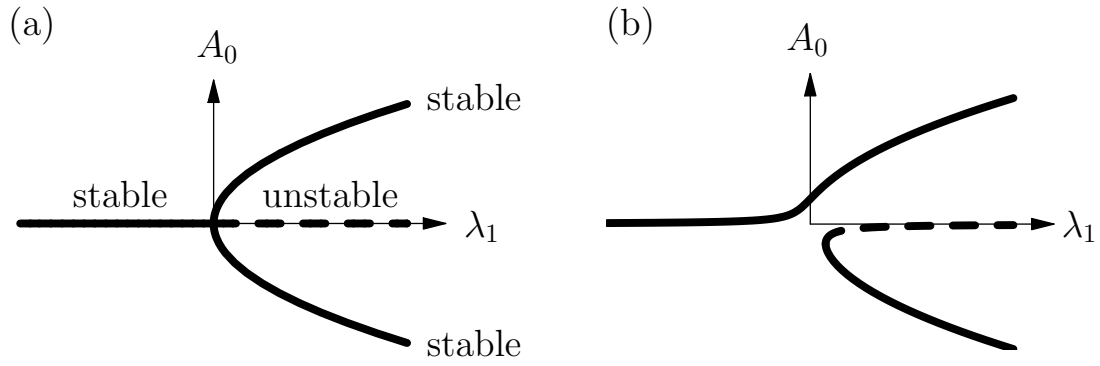


Figure 6.9: (a) Pitchfork bifurcation diagram of leading-order amplitude $A_0$ versus forcing parameter $\lambda_1$. (b) The corresponding diagram when asymmetry is introduced.

By substituting for $\Theta_0$ from (6.50), we obtain the following equation for the leading-order amplitude.

$$A_0 \left( A_0^2 - \frac{8\lambda_1}{n^2} \right) = 0. \tag{6.52}$$

When $\lambda_1$ is negative, the only real solution of (6.52) is $A_0 = 0$ but, for positive values of $\lambda_1$, there are three such solutions: $A_0 = 0, \pm(2/n)\sqrt{2\lambda_1}$. This behaviour of $A_0$ as a function of $\lambda_1$, depicted in Figure 6.9(a), is characteristic of a so-called *pitchfork bifurcation*.

Working backwards, we can easily turn (6.52) into an equation for the amplitude of $\theta$, that is

$$|A| \left[ |A|^2 - 8 \left( \frac{\lambda}{n^2} - 1 \right) \right] = 0, \tag{6.53}$$

and this weakly nonlinear response is plotted in Figure 6.8(b). This gives the physically expected result that the amplitude of each buckled solution increases with the excess applied force. We can also see how Figure 6.8(a) approximates this response for very small $|A|$. For comparison, we also show the response of the full nonlinear solution of (6.38).

We can use the argument after (6.22) to show that the solution $\theta = 0$ is stable for $\lambda_1 < 0$ but loses stability to the nonzero solution as $\lambda_1$ crosses zero, which justifies the labelling in Figure 6.9(a). Another key ingredient of bifurcation pictures like Figure 6.9(a) is the *symmetry* that we have assumed in our strut model. Any imperfection or asymmetry in the model, for example gravity acting in the transverse direction, would deform the response diagram into something like Figure 6.9(b), in which there is a smooth dependence of the solution on the control parameter.